Hybrid Operational Modal Analysis of an Operative Two-bladed Offshore Wind Turbine

D.W.B. ter Meulen

TU Delft

Image source: Seawind

HYBRID OPERATIONAL MODAL ANALYSIS OF AN OPERATIVE TWO-BLADED OFFSHORE WIND TURBINE

by

D.W.B. ter Meulen

to obtain the degree of Master of Science
at the Delft University of Technology,
to be defended publicly on Friday February 17, 2023 at 11:00 AM.

Student number:	4600355	
Project duration:	March 17, 2022 – February 17, 2023	
Thesis committee:	Dr. Ir. A. Cicirello,	TU Delft, chair
	Dr. Ir. A. Cabboi,	TU Delft
	Dr. Ir. A. Antonini,	TU Delft

An electronic version of this thesis is available at http://repository.tudelft.nl/.

TU Delft

ABSTRACT

Two-bladed offshore wind turbines regained interest in finding the most profitable way of generating wind energy. Wind industry companies demand the safe operation of two-bladed offshore wind turbines. To guarantee safe operation, the companies perform operational modal analyses to investigate modal properties variation which might be allocated to damage. However, the operational modal analysis of an operative two-bladed offshore wind turbine faces multiple challenges. (1) Fundamental operational modal analysis assumptions about the applied loads are violated by environmental and operational loads. (2) The closely spaced modes of an offshore wind turbine are hard to identify. (3) An operative two-bladed offshore wind turbine is a linear time-variant system. This paper introduces an enhanced operational modal analysis procedure to overcome some of the mentioned challenges. The enhanced procedure incorporates a post-processing technique in a transmissibility-based approach. A developed representative model of an operative two-bladed offshore wind turbine is used to compare the enhanced procedure with the frequency domain decomposition method. Based on the comparison, this paper proposes a new operational modal analysis method that combines a transmissibility-based approach, the post-processing technique, and the frequency domain decomposition method. This paper proves that this proposed combined method is a promising new operational modal analysis technique that outperforms the enhanced procedure and the frequency domain decomposition method in identifying the modal properties of a two-bladed offshore wind turbine.

D.W.B. ter Meulen
Rotterdam, February 2023

CONTENTS

1 INTRODUCTION

In recent years, renewable energy sources utilization has boosted the use of wind energy, resulting in more Offshore Wind Turbines (OWTs). Wind industry companies demand the safe operation of OWTs and use Operational Modal Analysis (OMA) techniques as a Structural Health Monitoring (SHM) strategy to guarantee safe operation. This research focuses on a specific OMA technique based on transmissibility functions (TOMA) for an operative two-bladed OWT. The introduction briefly introduces the topics OWTs, SHM, OMA, and TOMA, after which it presents the objective of the research.

1.1 OFFSHORE WIND TURBINES

World leaders have made various treaties concerning climate change in recent years. Examples are the Paris Agreement in 2015 to limit global warming below 2 degrees Celsius [1] and the European Green Deal to become the first continent with net-zero emission of greenhouse gasses in 2050 [2]. Renewable energy sources (wind, water, or solar) are essential to reach the climate change goals of these treaties [2]. The various treaties have boosted the development of renewable energy sources. The fraction of energy coming from renewable sources has more than doubled between 2004 and 2021 in the European Union [3]. The use of wind as a renewable energy source has, consequently, also increased in recent years and will increase further in coming years since the Dutch Government has announced to raise their offshore wind energy goal to 21 GW in 2030 [4].

The wind industry is developing more and larger offshore wind farms to achieve this offshore wind energy goal. Offshore wind farms are more popular than onshore wind farms because offshore can produce more electricity [5]. Moreover, the lack of inexpensive land to build on or visual pollution for residents does not obstruct their expansion [5]. The wind industry is searching for the most profitable way to develop offshore wind farms. Two-bladed OWTs regained interest in this exploration for multiple reasons. The most important motivation is that a two-bladed OWT shows almost similar efficiency as a three-bladed OWT but has significantly lower costs of materials, construction, and maintenance [6]. Therefore, two-bladed OWTs might dominate newly developed offshore wind farms [6].

Wind industry companies demand a safe operation of the two-bladed OWTs and want to know when maintenance is required to repair the OWTs or extend the service life of the OWTs. Digital monitoring controls the structural condition and damage to ensure safe operation and plan strategic activities that can extend the service life. Companies prefer digital monitoring of OWTs over visual monitoring since visual monitoring is dangerous for employees and more expensive for companies [7]. However, sensors cannot monitor the structural condition and damage directly. Strategies are necessary to retrieve information regarding the structural condition from measurements. Companies use SHM strategies to achieve this and to make decisions to guarantee the safe operation of two-bladed OWTs.

1.2 STRUCTURAL HEALTH MONITORING

SHM strategies are techniques implemented on a full-scale civil structure to provide information regarding the structural condition. Different SHM strategies exist, of which system identification-based approaches are well-known [8]. A branch of system identification, modal identification, identifies the modal properties of a structure, like the natural frequencies, damping ratios, and mode shapes. Modal identification is suitable for multi-purposes and can be used for, for example, damage identification and modal updating [9]. One damage identification method that relies on modal identification is tracking the structural modal properties over time to detect anomalies that can potentially indicate damage. One model updating strategy that relies on modal identification is updating the parameters of a numerical model based on identified modal properties.

Different methods to identify the modal properties of a civil structure exist, of which Experimental Modal Analysis (EMA) and OMA are commonly used [10]. EMA and OMA rely on the relationships of a dynamical system, simplified in Fig. 1.1, consisting of three components: the input, the object, and the output. The civil structure of interest represents the object, the applied loads on the structure represent the input, and the dynamic responses of the structure (like displacement, velocity, and acceleration) represent the output.

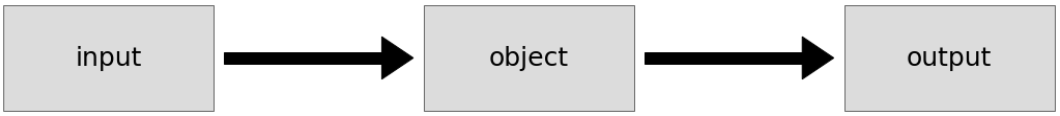

Figure 1.1: Dynamical system - simplified

EMA is a very accurate modal identification strategy. EMA uses input and output measurements of a structure to identify the modal properties. However, input measurements that define the applied loads are hardly available for civil structures, which makes EMA less suitable as a modal identification strategy for civil structures. OMA, on the other hand, uses output-only measurements. Therefore, OMA is more advantageous for the modal identification of civil structures because OMA requires no input data.

1.3 OPERATIONAL MODAL ANALYSIS

OMA is a promising technique for wind industry companies as an SHM strategy for the 2-bladed OWT since it requires output-only measurements. However, OMA faces some challenges in identifying and tracking the modal properties of an operative two-bladed OWT over time.

The first challenge is related to the loads applied to an operative OWT. OMA makes some assumptions regarding the applied loads, although no measurements are required. General assumptions are that the applied loads are uncorrelated white noise excitations acting over the entire structure. However, aerodynamic loads, hydrodynamic loads, and an operating rotor excite an operative OWT. These environmental and operational loads are non-white noise excitations that violate the fundamental OMA assumptions regarding the applied loads. The nature of environmental and operational loads causes potential misidentification of modal properties and limits the applicability of OMA for an operative OWT [11].

The second challenge is related to the modal properties of an OWT. OWTs have closely spaced modes because of their almost symmetrical shape. For example, the natural frequencies of the first tower bending modes in the fore-aft and side-side direction are often very close to each other [12]. Closely spaced modes complicate the identification of modal properties because closely spaced modes are more difficult to identify separately and correctly than well-separated modes using OMA techniques [10].

The third challenge is an interesting time-variant phenomenon that occurs and which is specific to an operative two-bladed OWT. In contrast to three-bladed OWTs, the modal properties of a two-bladed OWT change depending on the azimuthal angle of the blades [13]. An operative two-bladed OWT becomes a time-variant system due to the varying modal properties. OMA of a time-variant system is problematic because OMA techniques assume a linear time-invariant system. Therefore, the time-varying modal properties violate the fundamentals of OMA [10].

The mentioned challenges indicate the limited applicability of many existing OMA techniques to an operative two-bladed OWT. However, a relatively new method called TOMA is a promising opportunity that may overcome some of these limitations.

1.4 TRANSMISSIBILITY-BASED OPERATIONAL MODAL ANALYSIS

TOMA is a relatively new and promising technique that may be advantageous for the OMA of an operative two-bladed OWT for multiple reasons. TOMA makes no assumptions about the nature of the applied loads and can correctly identify the modal properties for non-white noise excitations [14]. Consequently, environmental and operational loads no longer violate fundamental assumptions, which reduces the possibility of incorrect identification of modal properties. Moreover, some TOMA approaches can identify closely spaced modes [15].

Multiple TOMA approaches exist, which are generally divided into two types. The classic formulation of Response Transmissibility (RT) and Power Spectral Density Transmissibility (PSDT) [14]. The most useful TOMA approach for an operative two-bladed OWT is a method that combines PSDT and Blind Source Separation (BSS) [15]. There are multiple reasons why the PSDT & BSS method is the best TOMA approach.

The PSDT & BSS method overcomes different challenges of OMA of an operative two-bladed OWT. Like every TOMA approach, the PSDT & BSS method can correctly identify the modal properties for non-white noise excitations. Besides, unlike traditional TOMA approaches, the PSDT & BSS method can identify closely spaced modes [15].

Moreover, PSDT techniques are more robust to noisy measurements and user-friendlier than RT techniques. PSDT techniques require only one dataset, while RT techniques require multiple datasets of different load cases [16].

Important to highlight as well is that an OWT satisfies the requirements of PSDT approaches regarding the applied loads. PSDT requires that at least two different loads excite the structure of interest. This requirement is satisfied for an OWT by the aerodynamic and hydrodynamic loads [16].

However, the PSDT & BSS method encounters limitations in identifying modal properties. Misidentifications of modal properties may occur in the presence of harmonic loads [17] and for non-fully loaded structures [18]. Scientists discovered opportunities to overcome these limitations. Do et al. [17] propose a post-processing step to deal with harmonic loads, and Araújo et al. [18] an enhanced procedure to tackle non-fully loaded structures.

This research goes one step further by incorporating the findings of both Do et al. [17] and Araújo et al. [18] in the PSDT & BSS method. In this way, a promising procedure is proposed that overcomes all mentioned limitations of the PSDT & BSS method. The proposed procedure is further mentioned as *the enhanced PSDT & BSS method* and is as follows:

1. Perform a closely spaced mode identification using a combined method of BSS [15] and the enhanced PSDT method [18]
2. Select candidate modal properties of the closely spaced mode identification
3. Assess the candidate modal properties using the post-processing tool of Do et al. [17]
4. Identify modal properties based on the assessment of candidate modal properties

1.5 RESEARCH OBJECTIVE

The research investigates the applicability of the enhanced PSDT & BSS method for an operative two-bladed OWT. Based on that, the following research objective is defined:

'Benchmark the performance of the enhanced PSDT & BSS method for an operative two-bladed OWT.'

A representative numerical model of an operative two-bladed OWT is developed to generate different dynamic responses. This research considers dynamic responses of a standstill OWT loaded by a coloured noise excitation, noise-contaminated dynamic responses of a standstill OWT excited by environmental loads, and noise-contaminated dynamic responses of an operative OWT excited by environmental and operational loads. The enhanced PSDT & BSS method is implemented and applied to identify modal properties from the generated dynamic responses. The identified modal properties are compared with the known modelled modal properties. A comparison is made between the suitability of the enhanced PSDT & BSS method and the generally used Frequency Domain Decomposition (FDD) [19] method to benchmark the enhanced PSDT & BSS method. Based on the comparison, this paper proposes a new OMA approach that combines the PSDT method, the post-processing step, and the FDD method to identify modal properties.

1.6 SET-UP REPORT

The report is organized as follows. Chapter 2 presents a paper that concisely describes the research. Chapter 3 reiterates the conclusions drawn in the paper and gives recommendations for future work.

2 PAPER

HYBRID OPERATIONAL MODAL ANALYSIS OF AN OPERATIVE TWO-BLADED OFFSHORE WIND TURBINE

Daan W.B. ter Meulen[1], **Alessandro Cabboi**[1], **Alice Cicirello**[1], **and Alessandro Antonini**[1]

[1] Delft University Of Technology
Faculty of Civil Engineering and Geosciences
Stevinweg 1, 2628 CN Delft, The Netherlands

Keywords: Two-bladed offshore wind turbine, Operational modal analysis, Transmissibility function

Abstract. *Two-bladed offshore wind turbines regained interest in finding the most profitable way of generating wind energy. Wind industry companies demand the safe operation of two-bladed offshore wind turbines. To guarantee safe operation, the companies perform operational modal analyses to investigate modal properties variation which might be allocated to damage. However, the operational modal analysis of an operative two-bladed offshore wind turbine faces multiple challenges. (1) Fundamental operational modal analysis assumptions about the applied loads are violated by environmental and operational loads. (2) The closely spaced modes of an offshore wind turbine are hard to identify. (3) An operative two-bladed offshore wind turbine is a linear time-variant system. This paper introduces an enhanced operational modal analysis procedure to overcome some of the mentioned challenges. The enhanced procedure incorporates a post-processing technique in a transmissibility-based approach. A developed representative model of an operative two-bladed offshore wind turbine is used to compare the enhanced procedure with the frequency domain decomposition method. Based on the comparison, this paper proposes a new operational modal analysis method that combines a transmissibility-based approach, the post-processing technique, and the frequency domain decomposition method. This paper proves that this proposed combined method is a promising new operational modal analysis technique that outperforms the enhanced procedure and the frequency domain decomposition method in identifying the modal properties of a two-bladed offshore wind turbine.*

2.1 INTRODUCTION

In recent years, two-bladed Offshore Wind Turbines (OWTs) regained interest in finding the most profitable way of generating wind energy due to similar efficiency but much lower costs than three-bladed OWTs [6]. Wind industry companies demand a safe operation of two-bladed OWTs and use Structural Health Monitoring (SHM) strategies to guarantee safe operation [8]. Commonly used SHM strategies rely on system identification. A branch of system identification, modal identification, identifies the modal properties of a structure, like the natural frequencies, damping ratios, and mode shapes [9]. Tracking the structural modal properties over time can detect anomalies that can potentially indicate damage. Different methods to identify modal properties exist, of which Experimental Modal Analysis (EMA) and Operational Modal Analysis (OMA) are the most well-known. EMA relies on input and output measurements, while OMA only on output measurements. Input data are, however, hardly available for civil structures. Therefore, OMA approaches are advantageous for the modal identification of OWTs because no input data are required [10].

Nevertheless, OMA faces some challenges in identifying and tracking the modal properties of an operative two-bladed OWT over time. Firstly, although no measurements are required, OMA makes some assumptions regarding the applied loads. The nature of environmental and operational loads acting on an operative two-bladed OWT violates these fundamental assumptions and limits the applicability of OMA for an operative OWT [11]. Secondly, an OWT has closely spaced modes. Closely spaced modes complicate the identification of modal properties because closely spaced modes are more difficult to identify separately and correctly than well-separated modes using OMA techniques [10]. Thirdly, in contrast to three-bladed OWTs, the modal properties of a two-bladed OWT change depending on the azimuthal angle of the blades [13]. An operative two-bladed OWT becomes a time-variant system due to the varying modal properties. OMA of a time-variant system is problematic because OMA techniques assume a linear time-invariant system [10].

A relatively new method, Transmissibility-based OMA (TOMA), is a promising opportunity that may overcome some of the mentioned limitations and be advantageous for the modal identification of an operative two-bladed OWT for multiple reasons. TOMA makes no assumptions about the nature of the applied loads and can correctly identify the modal properties for non-white noise excitations [14]. Consequently, environmental and operational loads no longer violate fundamental assumptions, which reduces the possibility of incorrect identification of modal properties. Multiple TOMA approaches exist, which are generally divided into two types. The classic formulation of Response Transmissibility (RT) and Power Spectral Density Transmissibility (PSDT) [14]. The most useful TOMA approach for an operative two-bladed OWT is a method that combines PSDT and Blind Source Separation (BSS) [15].

The PSDT & BSS method is the most useful TOMA approach because the PSDT & BSS method overcomes multiple challenges of an operative two-bladed OWT. Like every TOMA approach, the PSDT & BSS method can correctly identify the modal properties for non-white noise excitations. Besides, unlike traditional TOMA approaches, the PSDT & BSS method can identify closely spaced modes [15]. However, the PSDT & BSS method encounters limitations too in identifying modal properties. Misidentifications of modal properties may occur in the presence of harmonic loads [17] and for non-fully loaded structures [18]. Scientists discovered opportunities to overcome these limitations. Do et al. [17] propose a post-processing step to deal with harmonic loads, and Araújo et al. [18] an enhanced procedure to tackle non-fully loaded structures.

This paper goes one step further by incorporating the findings of both Do et al. [17] and Araújo et al. [18] in the PSDT & BSS method. In this way, a promising procedure is proposed

that overcomes all mentioned limitations of the PSDT & BSS method. The proposed procedure is further mentioned as *the enhanced PSDT & BSS method* and is as follows:

1. Perform a closely spaced mode identification using a combined method of BSS [15] and the enhanced PSDT method [18]
2. Select candidate modal properties of the closely spaced mode identification
3. Assess the candidate modal properties using the post-processing tool of Do et al. [17]
4. Identify modal properties based on the assessment of candidate modal properties

This paper benchmarks the performance of the enhanced PSDT & BSS method to identify modal properties from simulated dynamic responses. A representative numerical model of an operative two-bladed OWT is developed to generate different dynamic responses. This research considers dynamic responses of a standstill OWT loaded by a coloured noise excitation, noise-contaminated dynamic responses of a standstill OWT excited by environmental loads, and noise-contaminated dynamic responses of an operative OWT excited by environmental and operational loads. The enhanced PSDT & BSS method is implemented and applied to identify modal properties from the simulated dynamic responses. The identified modal properties are compared with the known modelled modal properties. A comparison is made between the suitability of the enhanced PSDT & BSS method and the generally used Frequency Domain Decomposition (FDD) [19] method to benchmark the enhanced PSDT & BSS method.

Based on the comparison, this paper proposes a new OMA approach that combines the PSDT method, the post-processing step, and the FDD method to identify modal properties. This paper proves that this new OMA approach (further mentioned as *the combined OMA method*) outperforms the enhanced PSDT & BSS method and the FDD method in identifying the modal properties of a two-bladed OWT. The combined OMA method overcomes challenges and benefits from the possibilities of both techniques. The combined OMA method shows that combining the advantages of multiple OMA techniques is a very appealing opportunity to identify modal properties correctly.

This paper is structured as follows. The FDD method and the enhanced PSDT & BSS method are revisited in Section 2.2. Section 2.3 prescribes the numerical model of an operative two-bladed OWT. Section 2.4 presents the modal identification results of the FDD method and the enhanced PSDT & BSS method. The combined OMA method is proposed and validated in Section 2.5. Finally, Section 2.6 concludes with the possibilities and limitations of the combined OMA method.

2.2 OMA TECHNIQUES

Section 2.2.1 and Section 2.2.2 prescribe the working principles of the FDD method and the enhanced PSDT & BSS method. Important to mention is that this research focuses on identifying the natural frequencies and mode shapes as modal properties. Therefore, Section 2.2.1 and Section 2.2.2 devote no attention to identifying damping ratios.

2.2.1 Frequency Domain Decomposition

This section briefly prescribes the working principle of the FDD method. More details of this technique are in the paper of Brincker et al. [19].

The relationship in the frequency domain between the measured dynamic responses $\mathbf{x}(t)$ and the applied loads $\mathbf{p}(t)$ is defined as

$$\mathbf{S}_{xx}(\omega) = \mathbf{H}(\omega)\mathbf{S}_{pp}(\omega)\mathbf{H}(\omega)^{*T} \tag{2.1}$$

where $\mathbf{S}_{xx}(\omega)$ and $\mathbf{S}_{pp}(\omega)$ are the auto/cross – Power Spectral Density (PSD) matrices of the dynamic responses and the applied loads, $\mathbf{H}(\omega)$ is the frequency response function of the system, and $*T$ is the conjugate transpose.

The FDD method assumes that the applied loads are uncorrelated white noise excitations acting over the entire structure. By this assumption, $\mathbf{S}_{pp}(\omega)$ becomes a constant diagonal matrix ($\mathbf{C}$), and $\mathbf{S}_{xx}(\omega)$ can be expressed as

$$\mathbf{S}_{xx}(\omega) = \mathbf{H}(\omega)\mathbf{C}\mathbf{H}(\omega)^{*T} \propto \mathbf{H}(\omega)\mathbf{H}(\omega)^{*T} \tag{2.2}$$

with the Singular Value Decomposition (SVD) given by

$$\mathbf{S}_{xx}(\omega) \propto \mathbf{H}(\omega)\mathbf{H}(\omega)^{*T} = \mathbf{U}(\omega)\mathbf{\Sigma}(\omega)\mathbf{V}(\omega)^{*T} = \mathbf{U}(\omega)\mathbf{\Sigma}(\omega)\mathbf{U}(\omega)^{*T} \tag{2.3}$$

where ($\mathbf{U}(\omega)$) and ($\mathbf{V}(\omega)$) are the left and right singular vector matrices, and $\mathbf{\Sigma}(\omega)$ is the singular value matrix. Equation (2.3) demonstrates that the left and right singular vector matrices of $\mathbf{S}_{xx}(\omega)$ are similar.

A superposition of modal coordinates is another way to express $\mathbf{S}_{xx}(\omega)$ as

$$\mathbf{S}_{xx}(\omega) = \mathbf{\Phi}\mathbf{S}_{zz}(\omega)\mathbf{\Phi}^{*T} \tag{2.4}$$

where $\mathbf{\Phi}$ is the structure's mode shapes matrix and $\mathbf{S}_{zz}(\omega)$ the auto/cross – PSD matrix in modal coordinates.

A comparison shows a relationship between the left singular vectors of Eq. (2.3) and the mode shapes of Eq. (2.4). Accordingly, the modal properties of a structure are identified by applying the SVD to the PSD matrices of the dynamic responses using the following procedure:

1. Estimate $\mathbf{S}_{xx}(\omega)$ of the dynamic response
2. Decompose $\mathbf{S}_{xx}(\omega)$ in singular values and vectors using the SVD
3. Identify natural frequencies from peaks of the singular value graph
4. Identify mode shapes from left singular vectors corresponding to the peak

2.2.2 Enhanced PSDT & BSS method

This section briefly prescribes the working principle of the enhanced PSDT & BSS method. More details of this technique are in the references [15, 17, 18, 20].

The transmissibility function is the ratio of two dynamic responses, $x_i(t)$ and $x_j(t)$. The PSDT is, accordingly, the ratio of responses $x_i(t)$ and $x_j(t)$ with respect to response $x_z(t)$ and estimated by

$$T_{ij}^{z}(\omega) = \frac{S_{x_i x_z}(\omega)}{S_{x_j x_z}(\omega)} \tag{2.5}$$

where $S_{x_i x_z}(\omega)$ is the cross PSD of $x_i(t)$ and $x_z(t)$.

Araújo and Laier [20] proposed to collect the PSDTs of dynamic responses measured at L locations in a so-called Power Spectral Density Transmissibility Matrix (PSDTM) given by

$$\left[\mathbf{T}_j(\omega)\right] = \begin{bmatrix} S_{x_1x_1}/S_{x_jx_1} & S_{x_1x_2}/S_{x_jx_2} & \dots & S_{x_1x_L}/S_{x_jx_L} \\ S_{x_2x_1}/S_{x_jx_1} & S_{x_2x_2}/S_{x_jx_2} & \dots & S_{x_2x_L}/S_{x_jx_L} \\ \vdots & \vdots & \ddots & \vdots \\ S_{x_Lx_1}/S_{x_jx_1} & S_{x_Lx_2}/S_{x_jx_2} & \dots & S_{x_Lx_L}/S_{x_jx_L} \end{bmatrix}_{LxL} \tag{2.6}$$

where the (ω) of $S_{x_1x_1}(\omega)$, for example, is omitted for convenience.

Araújo and Laier [20] proved that the PSDTM of Eq. (2.6) has, at natural frequencies, the unique property of a rank equal to 1 due to linearly dependent columns. Based on this finding, the authors introduce a procedure to identify modal properties using the SVD since second and larger singular values tend towards zero if a matrix's rank is 1. Natural frequencies can then be identified from peaks of a graph plotting the inverse of these singular values.

However, this technique fails to identify closely spaced modes because the PSDTM of Eq. (2.6) has, in the proximity of closely spaced modes, a rank larger than 1 due to linearly independent columns. To overcome this problem, Araújo et al. [15] propose the PSDT & BSS method that combines PSDT and BSS techniques.

BSS intends to decompose dynamic responses in multiple uncorrelated signals called sources. To do this, BSS assumes dynamic responses to be a combination of sources defined as

$$\mathbf{x}(t) = \mathbf{A}\mathbf{s}(t) \tag{2.7}$$

where $\mathbf{x}(t)$ is the dynamic response vector, $\mathbf{s}(t)$ the source vector, and $\mathbf{A}$ a static mixing matrix. A direct relationship exists between BSS and the dynamic responses' modal decomposition given by

$$\mathbf{x}(t) = \mathbf{\Phi}\mathbf{z}(t) \tag{2.8}$$

where $\mathbf{\Phi}$ is the structure's mode shapes matrix and $\mathbf{z}(t)$ the response vector in modal coordinates. The similarities between Eqs. (2.7) and (2.8) indicate the applicability of BSS for OMA. If BSS decomposes the dynamic responses correctly, the structure's mode shapes can be estimated directly using the mixing matrix.

Araújo et al. [15] suggest using Second Order Blind Identification (SOBI) as a BSS technique [21]. SOBI is applicable to identify closely spaced modes and is the most robust BSS method for non-fully loaded structures, according to Araújo et al. [15]. SOBI defines the mixing matrix $\mathbf{A}$, estimates the sources by

$$\mathbf{s}(t) = \mathbf{A}^{-1}\mathbf{x}(t) \tag{2.9}$$

and obtains the contribution of source q at all sensor locations given by

$$a_i^q(t) = \mathbf{A}(i,q)s_q(t) \tag{2.10}$$

where $s_q(t)$ is source q and $a_i^q(t)$ the contribution of source q at sensor location i.

Araújo et al. [15] propose to incorporate the obtained sources in a new PSDTM given by

$$\left[\mathbf{PT}_j^q(\omega)\right] = \begin{bmatrix} S_{x_1x_1}/S_{a_j^q a_1^q} & S_{x_1x_2}/S_{a_j^q a_2^q} & \dots & S_{x_1x_L}/S_{a_j^q a_L^q} \\ S_{x_2x_1}/S_{a_j^q a_1^q} & S_{x_2x_2}/S_{a_j^q a_2^q} & \dots & S_{x_2x_L}/S_{a_j^q a_L^q} \\ \vdots & \vdots & \ddots & \vdots \\ S_{x_Lx_1}/S_{a_j^q a_1^q} & S_{x_Lx_2}/S_{a_j^q a_2^q} & \dots & S_{x_Lx_L}/S_{a_j^q a_L^q} \end{bmatrix}_{LxL} \tag{2.11}$$

where, again, the (ω) is omitted for convenience.

The authors proved that the PSDTM of Eq. (2.11) contains only one natural frequency, corresponding to the vibration mode of source q and that the matrix has the unique property of a rank equal to 1 at the natural frequency. Therefore, the modal properties of the vibration mode of source q can be identified as prescribed by Araújo and Laier [20]. By doing this for multiple sources, the structure's modal properties can be obtained, including the closely spaced modes.

However, the PSDT & BSS method encounters some limitations in identifying modal properties. The PSDT & BSS method misidentifies modal properties if: (1) Deficient separation of sources occurs because the number of active modes is larger than the number of sensors [15]. (2) Deficient separation of sources occurs because the structure is non-fully loaded [15]. (3) Spurious modes are introduced by the PSDT & BSS method because the structure is non-fully loaded [18]. (4) Harmonic modes are present because the structure is excited by harmonic loads [17].

Araújo et al. [18] propose an enhanced PSDTM method to reduce the risk of introducing spurious modes for non-fully loaded structures. The method recommends a modified PSDTM given by

$$\left[\mathbf{T}_j(\omega)\right]^{++} = \sum_{i=1}^{k} \frac{1}{\sigma_i^j(\omega)} \mathbf{V}_i^j(\omega) \mathbf{U}_i^j(\omega)^{*T} \tag{2.12}$$

where $\sigma_i^j(\omega)$, $\mathbf{V}_i^j(\omega)$ and $\mathbf{U}_i^j(\omega)$ are the i-th singular value, right-singular vector, and left-singular vector of $\mathbf{T}_j(\omega)$, and k is the number of singular values used in the summation. The paper of Araújo et al. [18] prescribes how to determine k.

After that, to identify modal properties, the authors calculate a weighted average function by

$$\pi(\omega) = \frac{\sum_{j=1}^{L} \left(\sigma_1^j(\omega)\right)^2}{\sum_{j=1}^{L} \sigma_1^j(\omega)} \tag{2.13}$$

where $\sigma_1^j(\omega)$ is the first singular value of the modified PSDTM of Eq. (2.12) and L the number of measurement locations. Modal properties are identified subsequently from peaks of the weighted average graph.

Do et al. [17] use a post-processing step to deal with harmonic modes. The post-processing step filters a peak in the frequency domain and transforms the filtered peak back to the time domain. In the time domain, the kurtosis value and the histogram of the filtered peak are determined. The kurtosis value and histogram indicate if the peak is a structural or a harmonic mode [10]. A structural mode has a histogram with a Gaussian distribution shape and a kurtosis value close to 3 because the dynamic response of a structure tends to be Gaussian for every type of excitation by the central limit theorem. On the other hand, a harmonic mode has a histogram with in the middle a minimum and at two extremes two maxima and a kurtosis value of 1.5.

This paper incorporates the findings of Do et al. [17] and Araújo et al. [18] in the PSDT & BSS method and proposes the enhanced PSDT & BSS method. The procedure to identify modal properties using the enhanced PSDT & BSS method is as follows:

1. Assemble the PSDTM of Eq. (2.6) and determine the number of singular values k according to Araújo et al. [18]
2. Perform SOBI [21] and collect the mixing matrix **A** and $a_i^q(t)$ in line with Eq. (2.10)
3. Assemble the PSDTM of Eq. (2.11) for source q
4. Construct the modified PSDTM of Eq. (2.12) using k of step 1 and the PSDTM of step 3
5. Select peaks of the weighted average graph of Eq. (2.13)
6. Assess if a peak corresponds to a structural or harmonic mode using the post-processing tool of Do et al. [17]
7. Identify the natural frequency from the peak of the weighted average graph for peaks that are structural modes according to step 6
8. Identify the mode shape from the mixing matrix **A** for peaks that are structural modes according to step 6
9. Repeat steps 3 to 8 for all sources

2.3 NUMERICAL MODEL

A representative numerical model of an operative two-bladed OWT is developed to generate dynamic responses for different load cases. The numerical model is a simplified representation of an OWT that encounters environmental and operational loads, closely spaced modes, and time-varying modal properties.

Section 2.3.1 defines the numerical model's equations of motion. Section 2.3.2 briefly describes the two-bladed OWT structure, and Section 2.3.3 the different load cases considered in this research. Eventually, Section 2.3.4 specifies the generated dynamic responses.

2.3.1 Equations of motion

The equations of motion of the numerical model are expressed as

$$\mathbf{M}(t)\ddot{\mathbf{x}}(t) + \mathbf{C}(t)\dot{\mathbf{x}}(t) + \mathbf{K}(t)\mathbf{x}(t) = \mathbf{S_p}(t)\mathbf{p}(t) \tag{2.14}$$

where $\mathbf{M}(t)$, $\mathbf{C}(t)$, and $\mathbf{K}(t)$ are the OWT's mass, damping, and stiffness matrices, and $\mathbf{S_p}(t)$ and $\mathbf{p}(t)$ represent the applied loads on the OWT, and $\mathbf{x}(t)$ and its time derivatives are the OWT's dynamic responses. In Eq. (2.14), the equations of motion deviate from standard equations of motion by making the matrices time-dependent to include the OWT's time-varying structural behaviour.

2.3.2 Two-bladed OWT structure

The numerical model is a simplified two-bladed OWT structure, as shown in Fig. 2.1, consisting of the OWT's tower, Rotor-Nacelle Assembly (RNA), and a fixed connection. The 'NREL offshore 5-MW baseline wind turbine' of Jonkman et al. is used as a reference to obtain material and cross-sectional properties [12].

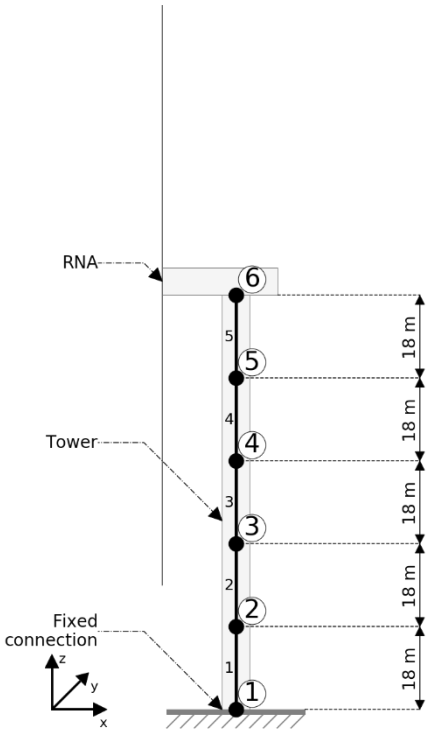

Figure 2.1: Simplified two-bladed OWT structure and its elements and nodes

The tower is modelled as a clamped cantilever beam of five two-node 3D Timoshenko beam elements [22]. 3D Timoshenko elements are used to include torsional and, more relevant for this research, closely spaced modes. Each element is a circular hollow steel section of 18 m in length, 6 m in diameter, and 0.027 m in thickness, with a density of 7850 kg/m^3. The assembly of five Timoshenko elements discretizes the tower into six nodes. Each node exists of six Degrees Of Freedom (DOFs): three translational and three rotational DOFs. The DOFs of the bottom node are removed to realize the clamped connection.

The RNA is modelled as a rigid-body mass matrix containing the RNA's mass and six inertial contributions. The rigid-body mass matrix is added directly to the top node of the tower. The mass is the weight of the nacelle (240000 kg), the hub (56780 kg), and the two blades (together 53411 kg), which are modelled as solid rectangular steel sections of 63 m in length,

0.45 m in width, and 0.12 m in thickness, with a density of 7850 kg/m^3. The six inertial contributions depend on the RNA's eccentricity (3.5 m) and the blades' azimuthal position.

Assembly of the tower elements and the RNA constructs the OWT's mass and stiffness matrices. The damping matrix is retrieved using a constant modal damping ratio of 1% for the first five modes. Higher modes are fully damped using a constant modal damping ratio of 100% to decrease the sampling frequency and, consequently, the computational time.

Table 2.1 presents the first five damped natural frequencies for a horizontal (0 degrees) and vertical (90 degrees) blade configuration. The natural frequencies vary depending on the blades' azimuthal position and the modes' sequence changes. For example, the torsional mode changes from a third position for the horizontal blade configuration to a fifth position for the vertical blade configuration. Figure 2.2 illustrates these phenomena in more detail for the first two damped natural frequencies. Table 2.1 and Fig. 2.2 prove that the numerical model has closely spaced modes and when the OWT is operative, time-varying modal properties.

Mode	Horizontal position [Hz]	Vertical position [Hz]
BM1 – SS	0.3291	0.3291
BM1 – FA	0.3358	0.3286
T	1.1641	4.3687
BM2 – SS	2.2351	2.2351
BM2 – FA	3.3101	2.1934

Table 2.1: Damped natural frequencies standstill OWT for horizontal and vertical blade configuration (BM = bending mode, T = torsional mode, SS = side-side direction, and FA = fore-aft direction)

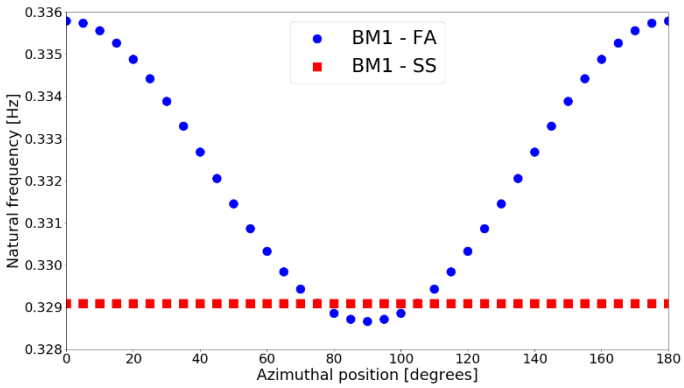

Figure 2.2: Damped natural frequencies mode 1 and 2 with respect to blades' azimuthal position

2.3.3 Load cases

The two-bladed OWT structure of Section 2.3.2 is used and excited by three different load cases, of which the complexity increases with each load case. Table 2.2 summarizes the three load cases, and Fig. 2.3 shows the spectra of the loads applied in the three load cases.

Load case	OWT configuration	Coloured noise excitation	Environmental loads	Operational load
LC1	Standstill	✓	×	×
LC2	Standstill	×	✓	×
LC3	Operative	×	✓	✓

Table 2.2: Load cases

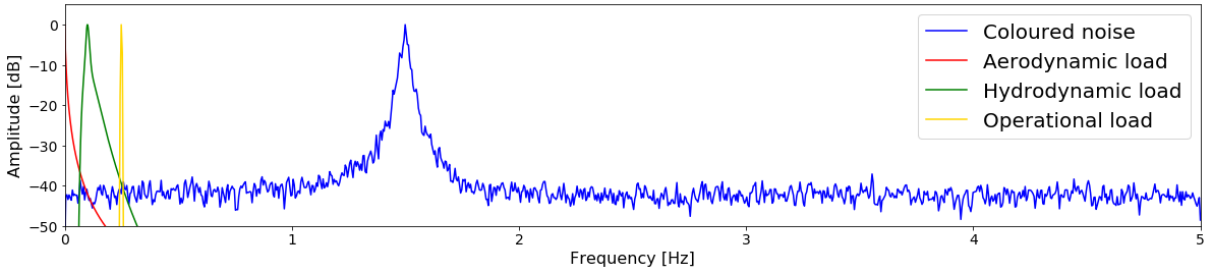

Figure 2.3: Spectra of coloured noise excitation, environmental loads (aerodynamic and hydrodynamic), and operational load

Load case 1 is a theoretical OWT (LC1) case to validate the implementation of the FDD method and the enhanced PSDT & BSS method. The OWT is in the standstill horizontal blade configuration. All nodes are loaded in the FA and the SS direction by uncorrelated coloured noise excitations with a predominant frequency of 1.5 Hz. The magnitude of the coloured noise excitation is four times larger in the FA direction than in the SS direction. Appendix A explains why the coloured noise excitation differs in magnitude in the FA and the SS direction.

Load case 2 is a standstill OWT (LC2) in the horizontal blade configuration excited by aerodynamic and hydrodynamic loads that violate OMA fundamentals. Two wind velocity time series, one in the FA direction and one in the SS direction, are simulated using the Kaimal spectrum [23] with a zero mean value, a 10-minute mean wind speed of 12 m/s at a reference height of 10 m and a turbulence intensity of 20%. The mean wind speed of 12 m/s at 10 m is added with a logarithmic profile over the tower's height to the time series in the FA direction. The aerodynamic loads of the wind velocity time series are calculated according to DNV-RP-C205 [24] and applied to the top four nodes in the FA and the SS direction. In addition, an irregular wave with an astronomical tide range of 3 m is simulated using the JONSWAP spectrum [23] with a significant wave height of 6 m and a peak period of 10 s. The direction of the irregular wave follows the wind velocity's direction. The hydrodynamic load and the point of application of the irregular wave are calculated according to DNV-RP-C205 using Stokes' second-order wave theory and Wheeler's stretching method [24]. The hydrodynamic load is applied to an extra node added in the bottom element that can move in time to deal with a time-varying point of application.

Load case 3 is an operative OWT (LC3) excited by operational and environmental loads that violate OMA fundamentals. Time-varying modal properties occur since the OWT is operative. The operational load is a harmonic load applied to the top node caused by an imbalance of the blades' masses. The magnitude of the harmonic load depends on the rotor speed, which is 15 rpm and constant over time. The environmental loads are the aerodynamic and hydrodynamic loads generated in the same way as the LC2's loads. However, LC3 modifies the aerodynamic load in the FA direction by including the blade passing effect of an operative OWT.

2.3.4 Dynamic responses

The equations of motion are solved using a discrete-time state-space model [10]. The solver assumes zero initial conditions and removes the first five minutes to mitigate the effect of the initial conditions. Moreover, the solver adds measurement noise to the dynamic responses of LC2 and LC3. The measurement noise is Gaussian noise with zero mean and a standard deviation of 10% of the dynamic responses' standard deviation.

Eventually, dynamic responses of 45 minutes with a sampling frequency of 10 Hz are generated for the three load cases, of which the responses of LC2 and LC3 are contaminated with noise.

2.4 NUMERICAL RESULTS

The translational dynamic responses in the FA and the SS direction of nodes 2 to 6, as shown in Fig. 2.1, are used to identify the two-bladed OWT's natural frequencies and mode shapes.

The focus is on identifying all modes for LC1 and the first two (closely spaced) modes for LC2 and LC3. Higher modes are disregarded for LC2 and LC3 since the environmental loads mainly excite the closely spaced modes.

The modal identification results of LC1 and LC2 are compared with the known modelled modal properties of the horizontal blade configuration of Table 2.1.

The FDD method and the enhanced PSDT & BSS method assume, to perform the modal identification, that LC3 is a linear time-invariant system. However, LC3 is not a linear time-invariant system due to the OWT's time-varying modal properties. To still account for the time-varying modal properties, this research compares the modal identification results of LC3 with the known modelled modal properties of both the horizontal and vertical blade configurations of Table 2.1.

Important to mention, already, is that torsional modes are not identified because the model cannot excite these modes due to a lack of spatial dimensions. Therefore, no attention is devoted to identifying the torsional modes.

Section 2.4.1 presents the results of the FDD method, and Section 2.4.2 the enhanced PSDT & BSS method. Both calculate the auto/cross – PSD matrices by Welch's method using a Fourier transform of size 2^{11}, 50% overlap, and a Hamming window of size 2^{11}.

2.4.1 Frequency Domain Decomposition

The results in Tables 2.3, 2.4, and 2.5 and Figs. 2.4 and 2.5 demonstrate that the FDD method can identify all excited modes of the two-bladed OWT for all three LCs, even the closely spaced modes. The identified natural frequencies are close to the modelled natural frequencies of Table 2.1, and the Modal Assurance Criterion (MAC) proves that the FDD method accurately estimates the mode shapes. However, the FDD method identifies additional peaks that do not belong to modal properties, like the 1.5 Hz coloured noise peaks for LC1 in Table 2.3 and Fig. 2.4, the environmental load peaks for LC2 in Table 2.4 and Fig. 2.5a, and the operational load peaks for LC3 in Table 2.5 and Fig. 2.5b.

Mode	Natural frequency [Hz]		Error [%]	MAC [-]
	Modelled	Identified		
BM1 – SS	0.3291	0.3271	0.59	0.99
BM1 – FA	0.3358	0.3369	0.33	1.00
*	-	1.4990	-	-
*	-	1.5088	-	-
BM2 – SS	2.2351	2.2412	0.27	1.00
BM2 – FA	3.3101	3.3203	0.31	1.00

Table 2.3: Numerical results LC1 using FDD (* = misidentification)

Mode	Natural frequency [Hz]		Error [%]	MAC [-]
	Modelled	Identified		
*	-	0.0977	-	-
*	-	0.1025	-	-
BM1 – SS	0.3291	0.3271	0.59	0.99
BM1 – FA	0.3358	0.3369	0.33	1.00

Table 2.4: Numerical results LC2 using FDD (* = misidentification)

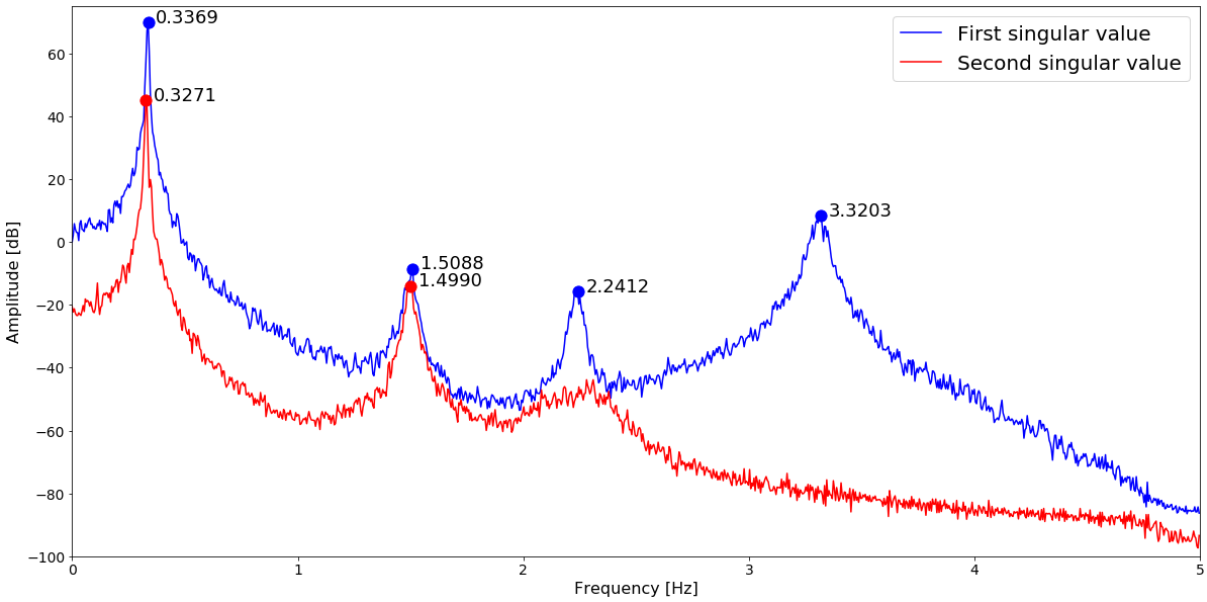

Figure 2.4: Numerical results LC1 using FDD

Mode	Natural frequency [Hz]			MAC [-]
	Horizontal	Vertical	Identified	
*	-	-	0.2490	-
*	-	-	0.2539	-
BM1 – SS	0.3291	0.3291	0.3271	1.00
BM1 – FA	0.3358	0.3286	0.3320	1.00

Table 2.5: Numerical results LC3 using FDD (* = misidentification)

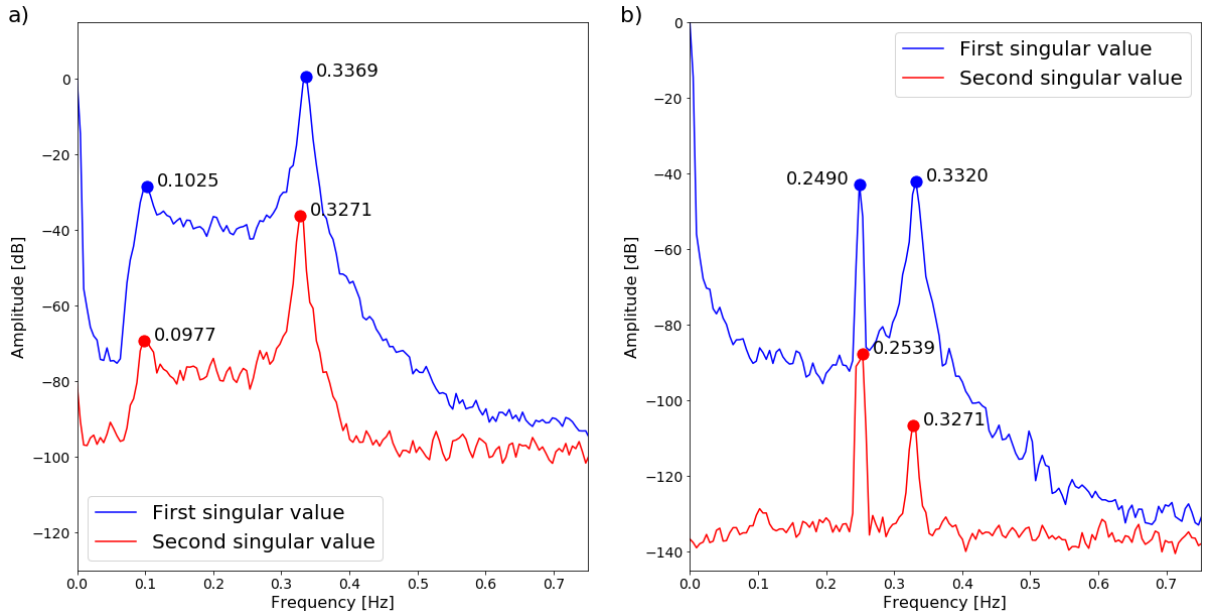

Figure 2.5: Numerical results using FDD: a) LC2; b) LC3

2.4.2 Enhanced PSDT & BSS method

Table 2.6 and Fig. 2.6 prove that the enhanced PSDT & BSS method identifies all excited modes of the two-bladed OWT for LC1. The identified natural frequencies are close to the modelled natural frequencies of Table 2.1, and the estimated mode shapes are accurate. Besides, the results are independent of the coloured noise excitation. The PSDT & BSS method does not identify an additional peak around 1.5 Hz like the FDD method in Fig. 2.4.

Mode	Natural frequency [Hz]		Error [%]	Kurtosis [-]	MAC [-]
	Modelled	Identified			
BM1 – SS	0.3291	0.3271	0.59	3.11	1.00
BM1 – FA	0.3358	0.3369	0.33	3.15	1.00
BM2 – SS	2.2351	2.2266	0.38	2.99	1.00
BM2 – FA	3.3101	3.3203	0.31	2.96	1.00

Table 2.6: Numerical results LC1 using enhanced PSDT & BSS

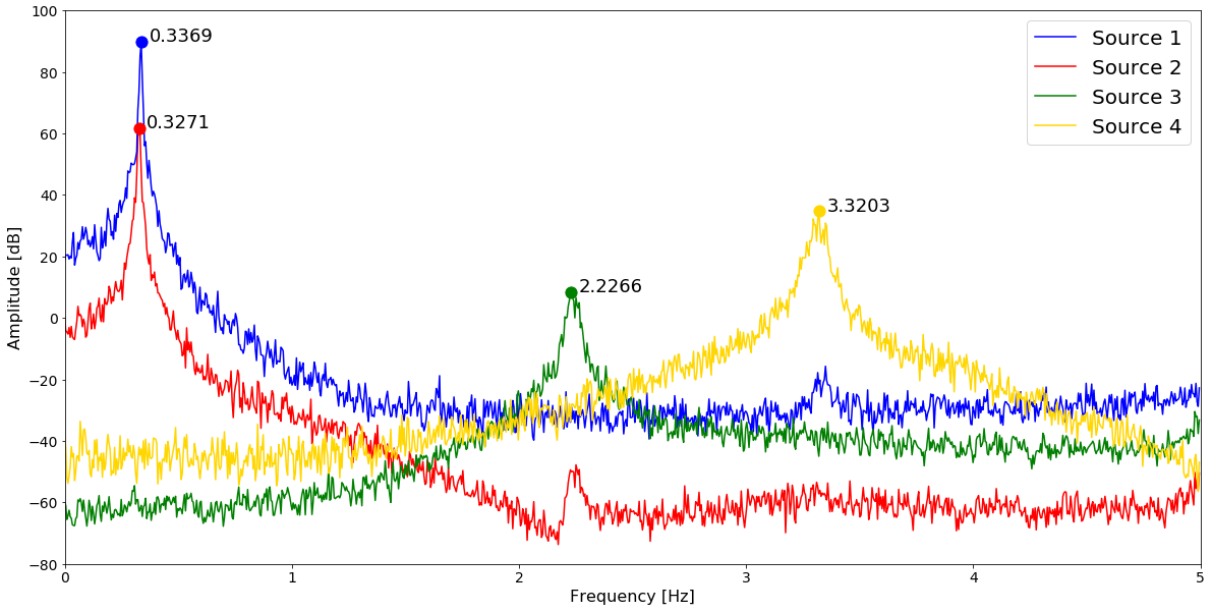

Figure 2.6: Numerical results LC1 using enhanced PSDT & BSS

However, Tables 2.7 and 2.8 and Fig. 2.7 show that the enhanced PSDT & BSS method identifies additional peaks for LC2 and LC3, like the environmental load peaks around 0.10 Hz and the operational load peak close to 0.25 Hz. The PSDT & BSS method cannot remove these peaks since the loads' spectra are non-wideband, as shown in Fig. 2.3 [16].

The kurtosis value and the histogram are used to assess if a peak corresponds to a structural or harmonic mode. The assessment results of the kurtosis value and the histogram go hand in hand. Therefore, only the kurtosis assessment is presented. The kurtosis assessment recognizes an operational load peak as a harmonic mode, as indicated in Table 2.8. However, the kurtosis assessment cannot separate the environmental load peaks from structural peaks, as shown in Tables 2.7 and 2.8.

Moreover, Table 2.7 shows an incorrect mode shape estimation of BM1 – SS for LC2. The enhanced PSDT & BSS method inadequately estimates the mode shape due to deficient mode separation caused by a non-fully loaded structure in LC2 [15]. The structure in LC2 is non-fully loaded because the loads considered in LC2 do not fully excite BM1 – SS.

A crucial remark is that, in this research, the number of sensors does not limit the use of the enhanced PSDT & BSS method. The number of sensors should be larger than the number of active modes to have sufficient separation. This research uses ten sensors, while the number of active modes is five at most due to the construction of the damping matrix.

Mode	Natural frequency [Hz]		Error [%]	Kurtosis [-]	MAC [-]
	Modelled	Identified			
*	-	0.0977	-	2.86	-
*	-	0.1074	-	2.89	-
BM1 – SS	0.3291	0.3271	0.59	2.92	0.54
BM1 – FA	0.3358	0.3369	0.33	2.95	1.00

Table 2.7: Numerical results LC2 using enhanced PSDT & BSS (* = misidentification)

Mode	Natural frequency [Hz]			Kurtosis [-]	MAC [-]
	Horizontal	Vertical	Identified		
*	-	-	0.1025	3.15	-
§	-	-	0.2490	1.50	-
BM1 – SS	0.3291	0.3291	0.3320	2.47	1.00
BM1 – FA	0.3358	0.3286	0.3320	2.47	1.00

Table 2.8: Numerical results LC3 using enhanced PSDT & BSS (* = misidentification, § = identified as harmonic peak by kurtosis assessment)

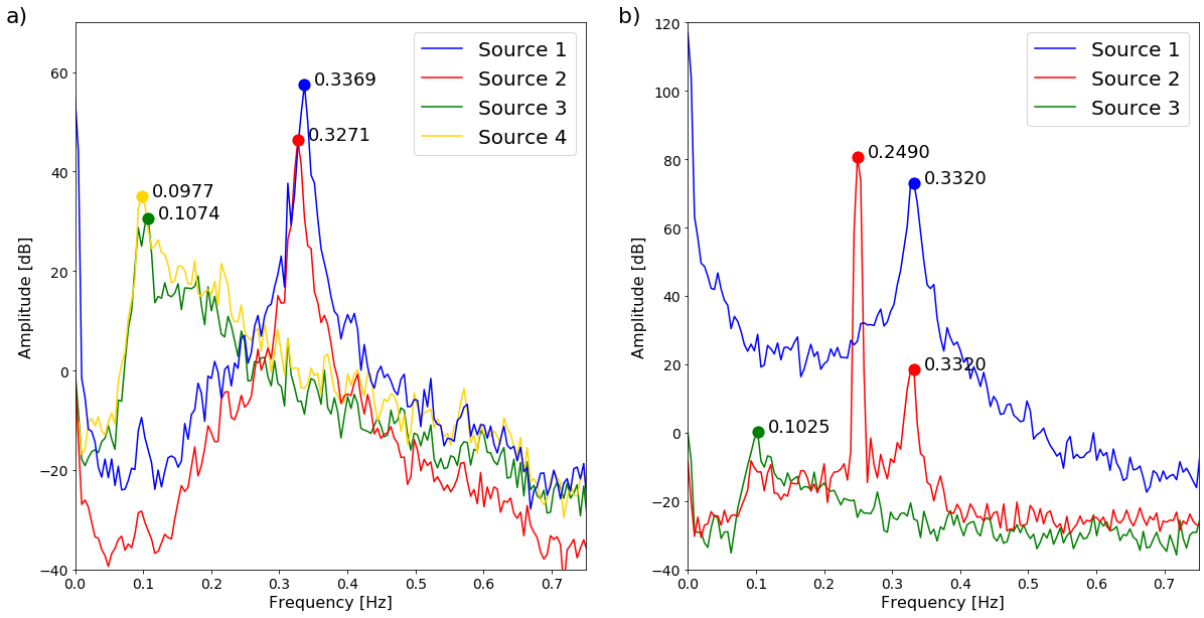

Figure 2.7: Numerical results using enhanced PSDT & BSS: a) LC2; b) LC3

2.5 PROPOSED COMBINED OMA METHOD

The results of Section 2.4.1 and Section 2.4.2 reveal that the FDD method and the enhanced PSDT & BSS method have possibilities and limitations in identifying modal properties of the two-bladed OWT. The FDD method accurately estimates the modal properties of the two-bladed OWT as long as there is pre-knowledge to distinguish structural peaks from applied load peaks. The enhanced PSDT & BSS method has the advantage of identification results independent of applied loads as long as these loads have a wideband spectrum. Moreover, the

approach separates harmonic peaks from structural peaks. Both capabilities of the enhanced PSDT & BSS method reduce the risk of misidentification of modal properties of the two-bladed OWT. However, the enhanced PSDT & BSS method requires a fully loaded structure for the correct identification of modal properties of the two-bladed OWT.

To overcome the limitations and still benefit from the advantages of both techniques, this research combines steps of the enhanced PSDT & BSS method and FDD method into the so-called *combined OMA method*.

The combined OMA method uses the PSDT method and the kurtosis assessment to reduce the risk of misidentification and the FDD method to identify closely spaced modes. The FDD method is preferred over the BSS method to identify closely spaced modes since the FDD method is user-friendlier and more robust for non-fully loaded structures. The proposed procedure of the combined OMA method to identify modal properties is as follows:

1. Perform the FDD method and select candidate modal properties according to Section 2.2.1
2. Assemble the PSDTM of Eq. (2.6) and determine the number of singular values k according to Araújo et al. [18]
3. Construct the modified PSDTM of Eq. (2.12) using k and the PSDTM of step 2
4. Select peaks of the weighted average graph of Eq. (2.13)
5. Assess if a peak corresponds to a structural or harmonic mode using the post-processing tool of Do et al. [17]
6. Identify the natural frequency and the mode shape from the FDD's candidate modal properties of step 1 for peaks that are structural modes according to step 5 *

* As explained in Section 2.2.2, the PSDT method cannot identify closely spaced modes. Therefore, one peak of step 4 may consist of closely spaced modes and can belong to multiple candidate modal properties.

The combined OMA method is used to identify the modal properties from generated dynamic responses of the two-bladed OWT for the three LCs of Section 2.3.3. The identification process is similarly performed as prescribed in Section 2.4.

The results in Tables 2.9, 2.10 and 2.11 and Figs. 2.8, 2.9 and 2.10 prove that the combined OMA method can identify all excited modes of the two-bladed OWT for all three LCs. The identified natural frequencies are close to the modelled natural frequencies of Table 2.1. Moreover, in contrast to the enhanced PSDT & BSS method, the combined OMA method obtains accurate estimations for all mode shapes, even for BM1 – SS of LC2, since the FDD method is used to estimate the mode shapes.

The results of LC1 are independent of the coloured noise excitation since the PSDT method removes this peak, as validated in Table 2.9 and Fig. 2.8.

Moreover, for LC3, the combined OMA method separates harmonic modes close to 0.25 Hz from structural modes using the kurtosis assessment, as demonstrated in Table 2.11.

Mode	Natural frequency [Hz]		Error [%]	Kurtosis [-]	MAC [-]
	Modelled	Identified			
BM1 – SS	0.3291	0.3271	0.59	3.15	0.99
BM1 – FA	0.3358	0.3369	0.33	3.15	1.00
¶	-	1.4990	-	-	-
¶	-	1.5088	-	-	-
BM2 – SS	2.2351	2.2412	0.27	2.96	1.00
BM2 – FA	3.3101	3.3203	0.31	2.90	1.00

Table 2.9: Numerical results LC1 using combined OMA (¶ = removed by PSDT)

However, for LC2, the combined OMA method misidentifies modal properties due to environmental loads. Table 2.10 and Fig. 2.9 show additional peaks close to 0.10 Hz. The PSDT method cannot remove the peak of the non-wideband hydrodynamic spectrum, and the kurtosis assessment cannot indicate the peak as a non-structural mode.

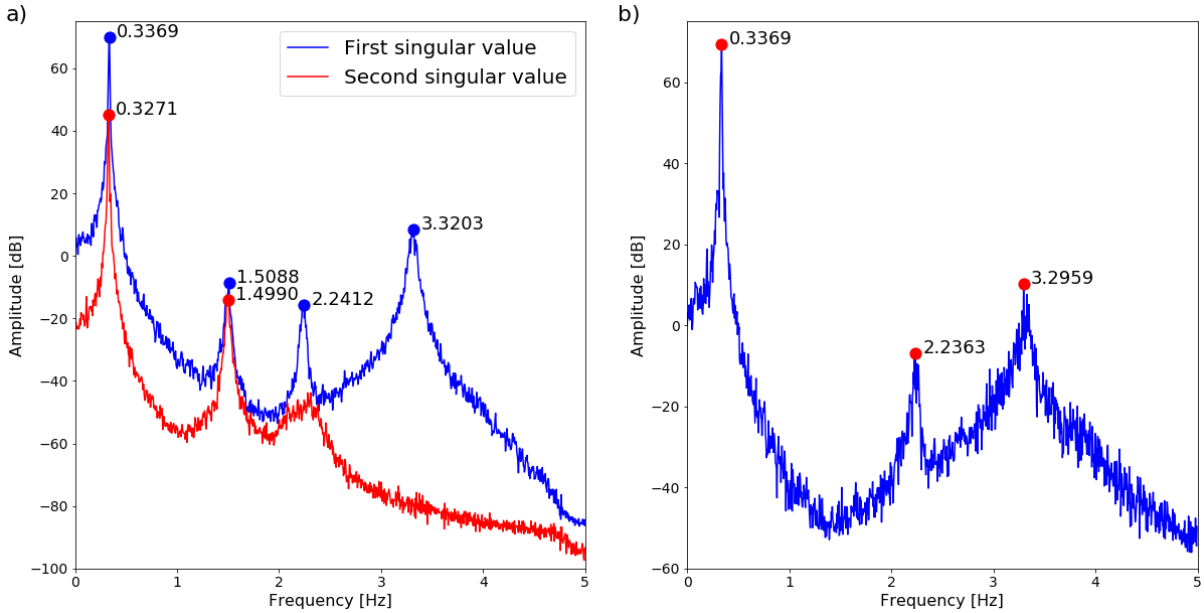

Figure 2.8: Numerical results LC1 using combined OMA: a) FDD; b) PSDT

Mode	Natural frequency [Hz]		Error [%]	Kurtosis [-]	MAC [-]
	Modelled	Identified			
*	-	0.0977	-	2.83	-
*	-	0.1025	-	2.83	-
BM1 – SS	0.3291	0.3271	0.59	2.95	0.99
BM1 – FA	0.3358	0.3369	0.33	2.95	1.00

Table 2.10: Numerical results LC2 using combined OMA (* = misidentification)

Mode	Natural frequency [Hz]			Kurtosis [-]	MAC [-]
	Horizontal	Vertical	Identified		
§	-	-	0.2490	1.50	-
§	-	-	0.2539	1.50	-
BM1 – SS	0.3291	0.3291	0.3271	2.47	1.00
BM1 – FA	0.3358	0.3286	0.3320	2.47	1.00

Table 2.11: Numerical results LC3 using combined OMA (§ = identified as harmonic peak by kurtosis assessment)

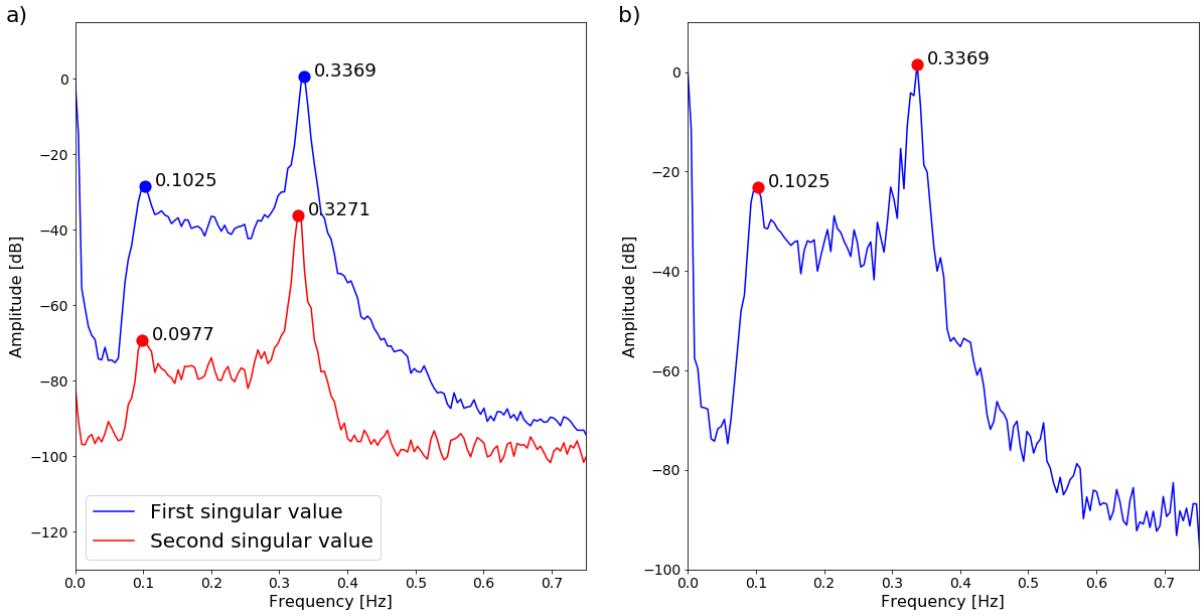

Figure 2.9: Numerical results LC2 using combined OMA: a) FDD; b) PSDT

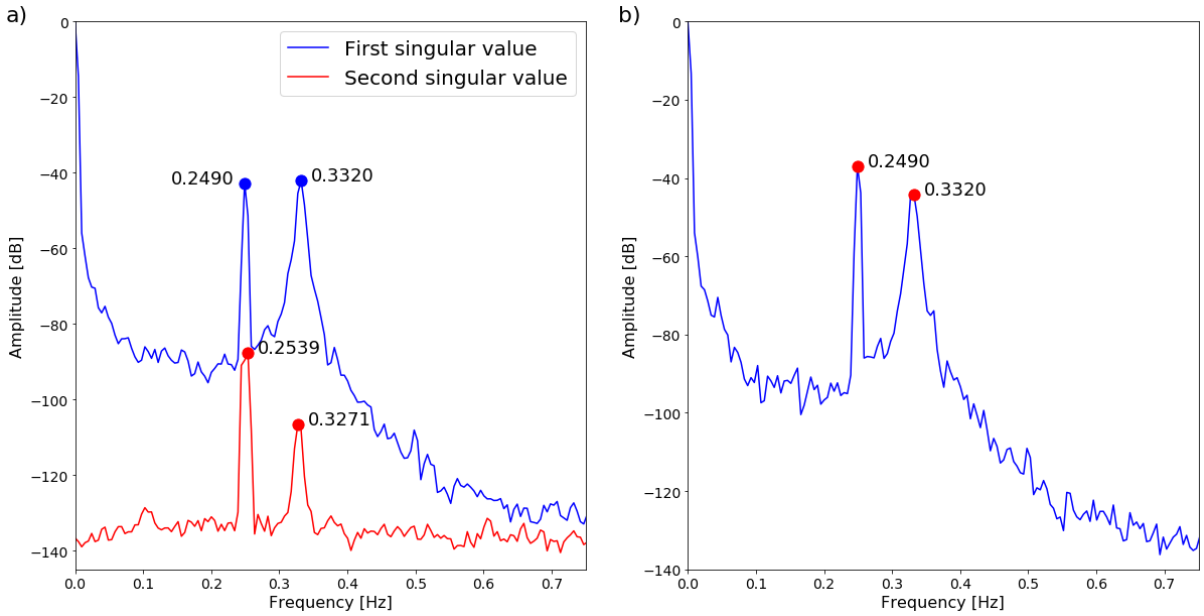

Figure 2.10: Numerical results LC3 using combined OMA: a) FDD; b) PSDT

2.6 CONCLUSIONS

Intending to identify modal properties from two-bladed OWT measurements, this research proposes a new OMA method that combines steps of the enhanced PSDT & BSS method and the FDD method into the so-called combined OMA method. The combined OMA method uses the PSDT method with the kurtosis assessment of the enhanced PSDT & BSS method and the closely spaced mode identification of the FDD method.

The combined OMA method is used to identify modal properties from dynamic responses generated by a representative model of a two-bladed OWT for three load cases to prove the applicability of the combined OMA method.

This research validates that the combined OMA method outperforms the FDD method and the enhanced PSDT & BSS method in identifying the modal properties of a two-bladed OWT.

The combined OMA method benefits from the advantages and overcomes the limitations of the FDD method and the enhanced PSDT & BSS method. In comparison to the FDD method, the combined OMA method reduces the possibility of misidentification in the presence of harmonic or coloured noise excitations. Moreover, unlike the enhanced PSDT & BSS method, the combined OMA method correctly estimates the mode shapes for non-fully loaded structures.

One drawback is that loads having a non-wideband or non-harmonic spectrum, like environmental loads, limit the use of the combined OMA method. The combined OMA method incorrectly identifies additional peaks from these loads as modal properties. Further research is necessary to overcome this limitation of the combined OMA method.

To conclude, this research shows that combining the advantages of different OMA methods is an attractive and promising direction to obtain more accurate and reliable modal identification results.

3 CONCLUSIONS AND RECOMMENDATIONS

This research aims to overcome the limited applicability of current OMA techniques to identify modal properties from measurements of an operative two-bladed OWT. This research proposes, to achieve this, a new OMA technique, the so-called combined OMA method (see Section 2.5). This chapter highlights the most important findings about the combined OMA method. Furthermore, this chapter gives recommendations for future work related to the combined OMA method.

3.1 CONCLUSIONS

The combined OMA method fuses steps of the FDD method (see Section 2.2.1) and the enhanced PSDT & BSS method (see Section 2.2.2). The combined OMA method uses the PSDT method with the kurtosis assessment of the enhanced PSDT & BSS method and the closely spaced mode identification of the FDD method.

The combined OMA method is used to identify modal properties from dynamic responses generated by a representative model of a two-bladed OWT for three load cases. The modal identification results of the combined OMA method are compared with the modal identification results of the FDD method and the enhanced PSDT & BSS method to prove the advantages of the combined OMA method.

The modal identification results of the combined OMA method are independent of wideband or harmonic excitation. This independency means that the combined OMA method reduces, in comparison to the FDD method, the possibility of misidentification in the presence of harmonic or coloured noise excitations. Moreover, unlike the enhanced PSDT & BSS method, the combined OMA method correctly estimates the mode shapes for non-fully loaded structures.

The comparison results show that the combined OMA method benefits from the advantages and overcomes the limitations of the FDD method and the enhanced PSDT & BSS method. Furthermore, the comparison validates that the combined OMA method outperforms the FDD method and the enhanced PSDT & BSS method in identifying modal properties of a two-bladed OWT.

One drawback is that loads having a non-wideband or non-harmonic spectrum, like environmental loads, limit the use of the combined OMA method. The combined OMA method incorrectly identifies additional peaks from these loads as modal properties. Further research is necessary to overcome this limitation of the combined OMA method.

To conclude, this research shows that combining the advantages of different OMA methods is an attractive and promising direction to obtain more accurate and reliable modal identification results.

3.2 RECOMMENDATIONS

This section emphasizes which further research is recommended to potentially overcome the limited applicability of the combined OMA method in the presence of loads having a non-wideband or non-harmonic spectrum.

The first recommendation to overcome the limitation is to use other TOMA approaches, like the RT-based methods. Multiple RT-based methods exist that are independent of all types of applied loads. The technique of Devriendt et al. [25] is an example of such a method. Loads having a non-wideband or non-harmonic spectrum can no longer limit the applicability of the combined OMA method if these RT-based methods are used. However, the RT-based methods have limitations as well. For example, the methods require at least two different load cases [16]. These limitations must be investigated thoroughly to see if RT-based methods are suitable for identifying modal properties of an operative two-bladed OWT.

The second recommendation to overcome the limitation is to use datasets of considerably different environmental conditions. The first step is to perform the modal identification using the combined OMA method for each dataset. Misidentifications may occur due to loads having a non-wideband or non-harmonic spectrum. The next step is to compare the modal identification results of each dataset. Based on this comparison, modal properties are distinguished from misidentifications since this recommendation assumes that misidentifications vary for each dataset while modal properties remain constant for each dataset. However, the drawback of this suggestion is that, in reality, modal properties vary over time as well due to, for example, changing temperatures. Therefore, the practical application of this suggestion may be limited.

This section has, in addition, some general recommendations related to the numerical model and the suitability of the combined OMA method for practical applications to consider in further research.

Interesting may be for further research to improve the numerical model. In this research, the numerical model is a simplified structure consisting only of the RNA, the tower, and the fixed connection. For further research, it may be valuable to consider more structural components of an OWT to have a more representative numerical model. In addition, the numerical model can be even more representative if a procedure is found to excite the torsional modes.

Moreover, it may be relevant to incorporate more types of time-varying structural behaviour of a two-bladed OWT. The numerical model considers only time-varying modal properties due to the rotation of the blades. However, in reality, different types of time-varying structural behaviour occur. For example, time-varying behaviour can occur due to changing temperatures. It will be interesting to see how the combined OMA method deals with these types of time-varying behaviour.

One last recommendation for further research is to validate the suitability of the combined OMA method for practical applications. This research proves the usefulness of the combined OMA method for a numerical experiment. However, it may be valuable to use real-field experimental data to validate the suitability of the combined OMA method for practical applications.

4 ACKNOWLEDGEMENT

Proudly, I present my master's thesis project to which I dedicated most of my time last year to obtain the degree of Master of Science in Civil Engineering at the Delft University of Technology. However, I could not achieve this without support. Therefore, I would like to thank the following people for their help:

First, I would like to express gratitude to my daily supervisor Alessandro Cabboi. He guided me through my master's thesis project and encouraged me to immerse myself in the intriguing topic of two-bladed OWTs. Moreover, Alessandro Cabboi was always ready to help me. I really appreciate his willingness to meet me every Monday between 11 AM – 12 AM.

In addition, I would like to express gratitude to my supervisors, Alice Cicirello and Alessandro Antonini. During progress meetings, Alice Cicirello and Alessandro Antonini provided me with new insights and feedback that helped me a lot to get the most out of my project. Therefore, I am happy that Alessandro Antonini will supervise during my PhD.

Finally, I would like to thank my family and friends for their confidence and unconditional support in finishing my master's thesis project.

A LOADS FA AND SS DIRECTION

The loads applied to the OWT differ in magnitude in the FA and the SS direction for all load cases. For example, the coloured noise magnitude is four times larger in the FA direction than in the SS direction. This appendix explains that a limited data length causes this difference in magnitude.

Welch's method is used to estimate auto/cross – PSD matrices. The sampling frequency, the segment length, the number of segments, and the overlap between two segments are critical components of Welch's method. This research fixes the sampling frequency at 10 Hz, the overlap between two segments at 50% and the minimum number of averages at 25 averages.

The only component to be determined is the segment length. The segment length is closely related to the frequency resolution and the dataset length. The larger the segment, the higher the frequency resolution and the larger the dataset. The segment length is handled with great care to identify modal properties. Natural frequencies of closely spaced modes are not distinguished if the frequency resolution is too low due to too few data points in a segment.

In this appendix, the FDD method identifies modal properties for varying segment lengths to investigate the influence of the segment length on modal identification. Modal properties are identified from dynamic responses of the standstill horizontal blade OWT configuration with modal properties of Table 2.1. Ten uncorrelated white noise excitations load the OWT, five in the FA direction and five in the SS direction. All white noise excitations have a zero mean and 100 N standard deviation.

The modal properties of the horizontal blade OWT configuration in Table 2.1 are used to decide the segment length. A minimum of 2^{11} data points is required to separate the closely spaced modes for a sampling frequency of 10 Hz. Consequently, a dataset of 45 minutes is required to have 25 averages that overlap 50%. Table A.1 and Fig. A.1 show the modal identification results using a 45-minute dataset and 2^{11} data points. Table A.1 and Fig. A.1 expose that the closely spaced modal identification is not as expected. The weak mode of the closely spaced modes has a biased mode shape estimation. A higher frequency resolution is required to distinguish the closely spaced modes.

Mode	Natural frequency [Hz]		Error [%]	MAC [-]
	Modelled	Identified		
BM1 – SS	0.3291	0.3320	0.89	0.24
BM1 – FA	0.3358	0.3369	0.33	0.98
BM2 – SS	2.2351	2.2412	0.27	1.00
BM2 – FA	3.3101	3.3203	0.31	1.00

Table A.1: Modal identification using 2^{11} data points

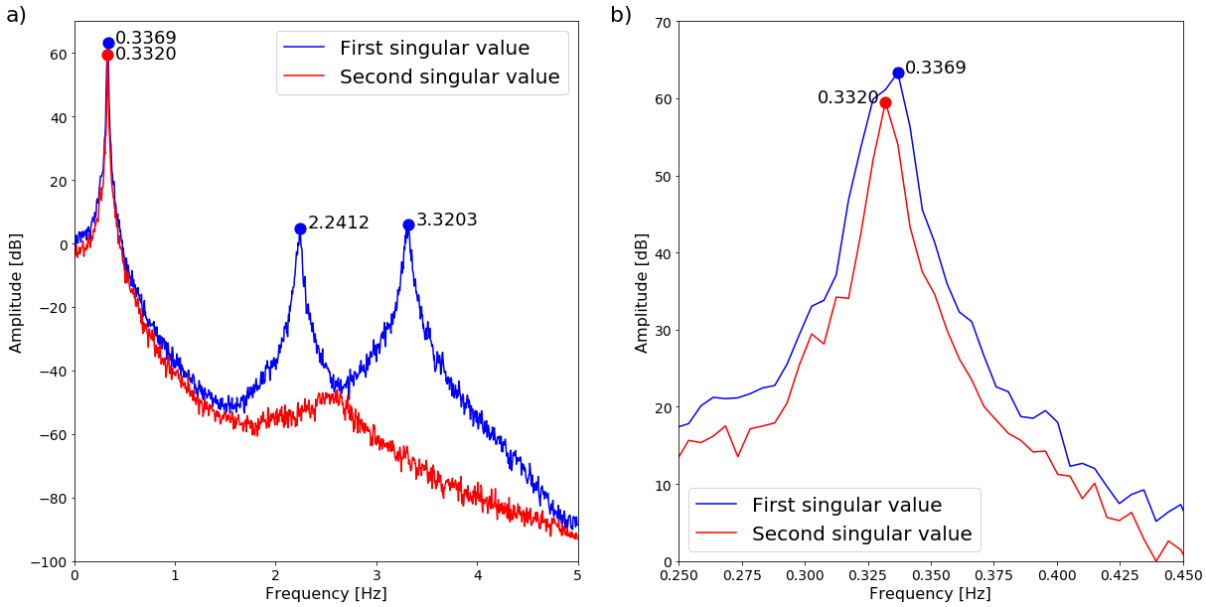

Figure A.1: Modal identification using 2^{11} data points: a) all identified modes; b) close-up of closely spaced modes

After an investigation, 2^{13} data points as segment length are suggested. A 3-hour dataset is generated to have 25 averages that overlap 50%. Table A.2 and Fig. A.2 show the modal identification results using 2^{13} data points and a dataset of 3 hours. Table A.2 and Fig. A.2 prove that closely spaced modes are identified using 2^{13} data points.

Mode	Natural frequency [Hz]		Error [%]	MAC [-]
	Modelled	Identified		
BM1 – SS	0.3291	0.3296	0.15	0.99
BM1 – FA	0.3358	0.3369	0.33	0.99
BM2 – SS	2.2351	2.2339	0.05	1.00
BM2 – FA	3.3101	3.3008	0.28	1.00

Table A.2: Modal identification using 2^{13} data points

These results pose a problem because a dataset of 3 hours is not feasible for an OWT, and shorter time series give biased mode shape estimations.

Loads with different magnitudes in the FA and the SS direction are applied to mitigate this problem. Rainieri and Fabbrocino [10] prescribe that the error of a biased mode shape estimation decreases if the difference between the first and second singular values becomes larger. The different magnitudes of the loads increase the difference between the first and second singular values. Therefore, the error of the weak mode shape's estimation decreases.

Table A.3 and Fig. A.3 show the modal identification results using 2^{11} data points and a 45-minute dataset when the white noise excitation has a four times larger magnitude in the FA direction than in the SS direction. Table A.3 and Fig. A.3 prove that the weak mode is estimated correctly when different magnitudes are used.

A different magnitude in the FA and the SS direction can be justified for an OWT since OWTs, in practice, are mainly loaded perpendicular to blades. Realistic loading behaviour still occurs for different magnitudes in both directions. Therefore, the difference in magnitude is applied to all load cases as prescribed in Section 2.3.3.

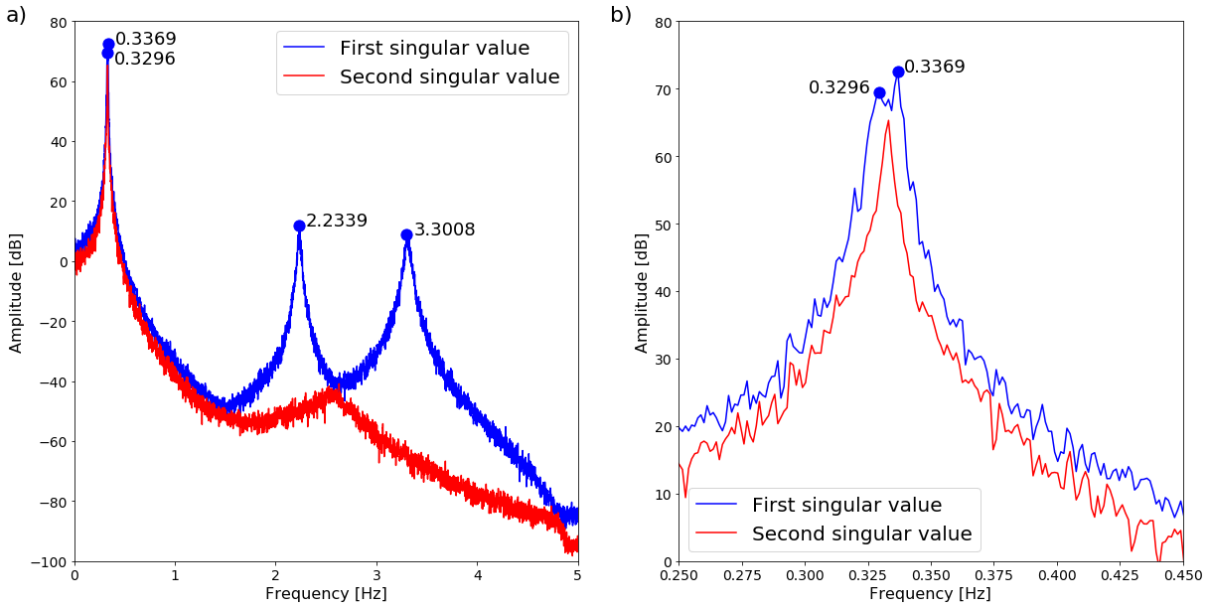

Figure A.2: Modal identification using 2^{13} data points: a) all identified modes; b) close-up of closely spaced modes

Mode	Natural frequency [Hz]		Error [%]	MAC [-]
	Modelled	Identified		
BM1 – SS	0.3291	0.3271	0.59	0.99
BM1 – FA	0.3358	0.3369	0.33	1.00
BM2 – SS	2.2351	2.2314	0.16	1.00
BM2 – FA	3.3101	3.3203	0.31	1.00

Table A.3: Modal identification using different magnitudes and 2^{11} data points

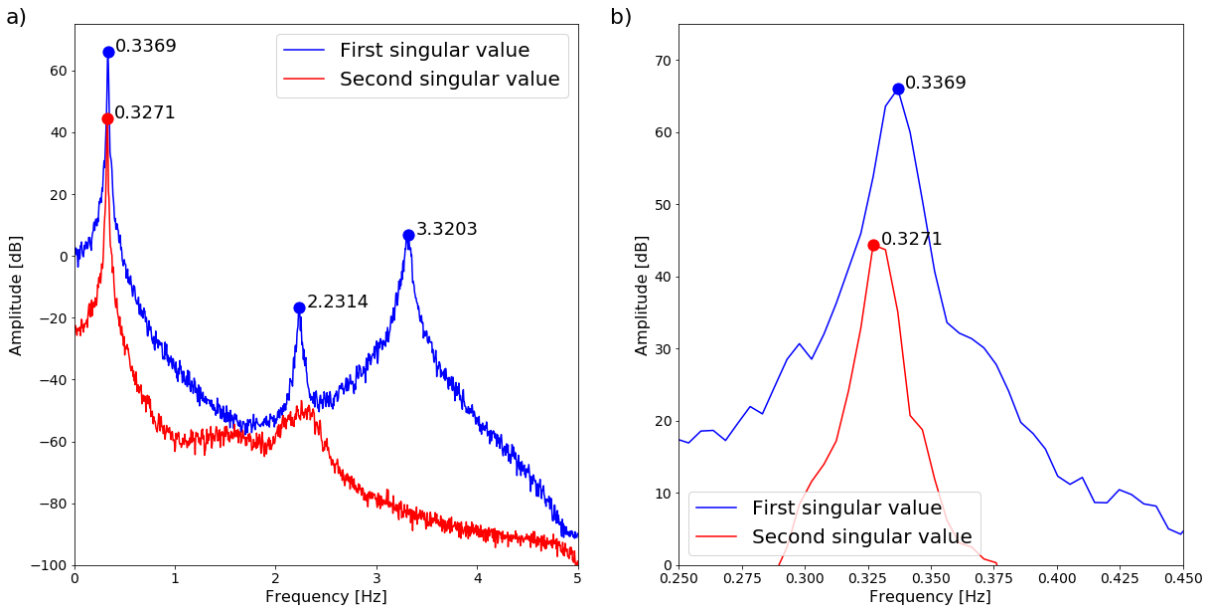

Figure A.3: Modal identification using different magnitudes and 2^{11} data points: a) all identified modes; b) close-up of closely spaced modes

REFERENCES

[1] UNFCCC. (2015). Paris Agreement. https://unfccc.int/sites/default/files/english_paris_agreement.pdf

[2] European Commission. (2019). The European Green Deal. https://eur-lex.europa.eu/legal-content/EN/TXT/?uri=CELEX:52019DC0640

[3] Eurostat. (2022). Renewable energy statistics. Eurostat - Statistics Explained. https://ec.europa.eu/eurostat/statistics-explained/index.php?title=Renewable_energy_statistics

[4] New Offshore Wind Energy Roadmap | RVO.nl. (n.d.). https://english.rvo.nl/information/offshore-wind-energy/new-offshore-wind-energy-roadmap

[5] Bilgili, M., Yasar, A., & Simsek, E. (2011). Offshore wind power development in Europe and its comparison with onshore counterpart. Renewable and Sustainable Energy Reviews, 15(2), 905–915. https://doi.org/10.1016/j.rser.2010.11.006

[6] WES - Wind Energy Solutions. (2020, November 30). How many blades are best for wind energy production? WES, Wind Energy Solutions. https://windenergysolutions.nl/uncategorized/how-many-blades/

[7] Karanikas, N., Steele, S., Bruschi, K., Robertson, C., Kass, J., Popovich, A., & MacFadyen, C. (2021). Occupational health hazards and risks in the wind industry. Energy Reports, 7, 3750–3759. https://doi.org/10.1016/j.egyr.2021.06.066

[8] Brownjohn, J. (2006). Structural health monitoring of civil infrastructure. Philosophical Transactions of the Royal Society A: Mathematical, Physical and Engineering Sciences, 365(1851), 589–622. https://doi.org/10.1098/rsta.2006.1925

[9] Catbas, F. N., Aktan, A. E., & Kijewski-Correa, T. L. (2013). Structural Identification of Constructed Systems: Approaches, Methods, and Technologies for Effective Practice of St-Id. American Society of Civil Engineers.

[10] Rainieri, C., & Fabbrocino, G. (2014). Operational Modal Analysis of Civil Engineering Structures: An Introduction and Guide for Applications (2014th ed.). Springer.

[11] Tcherniak, D., Chauhan, S., & Hansen, M. H. (2011). Applicability Limits of Operational Modal Analysis to Operational Wind Turbines. Structural Dynamics and Renewable Energy, Volume 1, 317–327. https://doi.org/10.1007/978-1-4419-9716-6_29

[12] Jonkman, J., Butterfield, S., Musial, W., & Scott, G. (2009). Definition of a 5-MW Reference Wind Turbine for Offshore System Development. National Renewable Energy Laboratory. https://doi.org/10.2172/947422

[13] Larsen, T. J., & Kim, T. (2016). Experimental and Numerical Study of Rotor Dynamics of a Two- and Three-Bladed Wind Turbine. International Journal of Offshore and Polar Engineering, 26(4), 355–361. https://doi.org/10.17736/ijope.2016.mmr12

[14] Yan, W. J., Zhao, M. Y., Sun, Q., & Ren, W. X. (2019). Transmissibility-based system identification for structural health Monitoring: Fundamentals, approaches, and applications. Mechanical Systems and Signal Processing, 117, 453–482. https://doi.org/10.1016/j.ymssp.2018.06.053

[15] Araújo, I. G., Sánchez, J. A. G., & Andersen, P. (2018). Modal parameter identification based on combining transmissibility functions and blind source separation techniques. Mechanical Systems and Signal Processing, 105, 276–293. https://doi.org/10.1016/j.ymssp.2017.12.016

[16] Kang, J., Ju, H., & Liu, L. (2021). Comparison of response transmissibility and power spectral density transmissibility on operational modal analysis. Mechanical Systems and Signal Processing, 160, 107912. https://doi.org/10.1016/j.ymssp.2021.107912

[17] Do, V. D., Le, T. P., & Beakou, A. (2019). Operational modal analysis of mechanical systems using transmissibility functions in the presence of harmonics. Journal of Science and Technology in Civil Engineering (STCE) - NUCE, 13(3), 1–14. https://doi.org/10.31814/stce.nuce2019-13(3)-01

[18] Gómez Araújo, I., Laier, J. E., & Carrazedo, R. (2019). Enhanced Power Spectral Density Transmissibility Matrix for Operational Modal Analysis of Structures. Journal of Structural Engineering, 145(6). https://doi.org/10.1061/(asce)st.1943-541x.0002322

[19] Brincker, R., Zhang, L., & Andersen, P. (2001). Modal identification of output-only systems using frequency domain decomposition. Smart Materials and Structures, 10(3), 441–445. https://doi.org/10.1088/0964-1726/10/3/303

[20] Araújo, I. G., & Laier, J. E. (2014). Operational modal analysis using SVD of power spectral density transmissibility matrices. Mechanical Systems and Signal Processing, 46(1), 129–145. https://doi.org/10.1016/j.ymssp.2014.01.001

[21] Belouchrani, A., Abed-Meraim, K., Cardoso, J. F., & Moulines, E. (1997). A blind source separation technique using second-order statistics. IEEE Transactions on Signal Processing, 45(2), 434–444. https://doi.org/10.1109/78.554307

[22] Panzer, H., Hubele, J., Eid, R., & Lohmann, B. (2009). Generating a Parametric Finite Element Model of a 3D Cantilever Timoshenko Beam Using Matlab. Lehrstuhl Für Regelungstechnik. https://mediatum.ub.tum.de/1072355

[23] Branlard, E. (2010). Generation of time series from a spectrum. TU Denmark. http://emmanuel.branlard.free.fr/work/papers/html/2010wral4/Branlard-2010-WindTimesSeriesGeneration.pdf

[24] Det Norske Veritas. (2010). Environmental conditions and environmental loads. In DNV-RP-C205.

[25] Devriendt, C., Weijtjens, W., De Sitter, G., & Guillaume, P. (2013). Combining multiple single-reference transmissibility functions in a unique matrix formulation for operational modal analysis. Mechanical Systems and Signal Processing, 40(1), 278–287. https://doi.org/10.1016/j.ymssp.2013.04.008